Light emitting diodes using $In_xGa_{1-x}P$ quantum well structures for increasing the effectiveness of wound healing

Kaitlyn Parsons[1,2]

[1]*Department of Electrical and Computer Engineering*
[2]*Beckman Institute*
University of Illinois at Urbana-Champaign, Urbana, IL 61801, USA

ABSTRACT

Dermatology utilizes light therapy to treat skin injuries and wound healing, however, the traditional methods of skin irradiation using solar and ultraviolet light result in thermal damage [1]. The monochromatic wavelength of non-ablative laser therapy mitigates thermal damage. Despite this advantage, non-ablative laser therapy is impractical due to the immobility and the cost of the system [2]. Light emitting diodes offer a middle ground for tissue repair with the relatively narrow wavelength spectrum required for non-thermal treatment as well as mobility and cost advantages compared to laser therapy.

This project uses Crosslight TCAD software to investigate material effects on LED device performance for wavelength operation in the range of 610 to 650 nm. The LED device structure is comprised of $In_xGa_{1-x}P$ multiple quantum wells and $(Al_{0.6}Ga_{0.4})_{0.5}In_{0.5}P$ barriers. The quantum well indium composition, the number of quantum wells in the active region and the well thickness are studied. In particular, the effects of these parameters on the emission peak wavelength and intensity, the internal quantum efficiency, the I-V characteristic, and radiative recombination are studied. The indium composition of the quantum well material is varied between 40 – 70%. The number off quantum wells in the active region studied range between 1-10 wells. The effects of well thickness for a one quantum well structure are studied. Optimization of these parameters will increase the effectiveness of light therapy for patients afflicted with skin wounds and injuries.

1. INTRODUCTION AND MOTIVATION

Skin is comprised of multiple tissue layers that serve as protection from microbes and the outside environment as well as provide temperature regulation for the body [3]. A wound describes a discontinuity in the skin tissue due to injury [4]. Difficult to heal wounds create emotional stress in patients, thereby degrading the quality of life for the injured patient [4]. Innovative technology is required to decrease the difficulty of wound healing. Intense research toward light therapy wound healing will enable a reduction in infection risk and costs of wound dressings for the patient as well as reduce costs and resources for health care facilities. Light in the wavelength range of 600 nm to 1000 nm stimulates cellular tissues growth [5]. In 2011, Fushimi *et al* demonstrated the effectiveness of LED light therapy for superficial wounds in mice [1]. However, study in device design for specific emission ranges is necessary. Specifically, the effects of wavelengths in the 610 nm to 650 nm using $In_xGa_{1-x}P$ multiple quantum wells for wound healing requires further study.

The top epidermis layer has a rough side, called the stratum corneum (*FIGURE 1*) [6]. This layer has direct contact to the elements of the environment and maintains a waterproof barrier between the environment and the body [7]. The dermis is the middle layer containing hair follicles and connective tissue. The subcutaneous tissue layer is comprised of connective tissue and fat tissue. Different wavelengths of

light penetrate to different layers of the skin. Blue wavelengths (450 – 495 nm) only infiltrate the epidermis. Adamskaya *et al* demonstrated the effectiveness of blue LEDs for healing wounds to the top epidermis layer in mice [8]. The results are that blue wavelength light significantly improved the rat and quality in healing wounds in the top layer of the skin. Red wavelengths (620 – 750 nm) infiltrate both the epidermis and the dermis and infrared wavelengths (750 – 1000 nm) infiltrate the skin all the way to the subcutaneous tissue layer. Wounds are classified by depth into the skin [9]. Superficial wounds refer to wounds only involving the epidermis. Both partial thickness and full thickness wounds involve both the epidermis and dermis. Thus, in order to heal partial thickness and full thickness skin wounds, LEDs with wavelengths in the red regime are necessary.
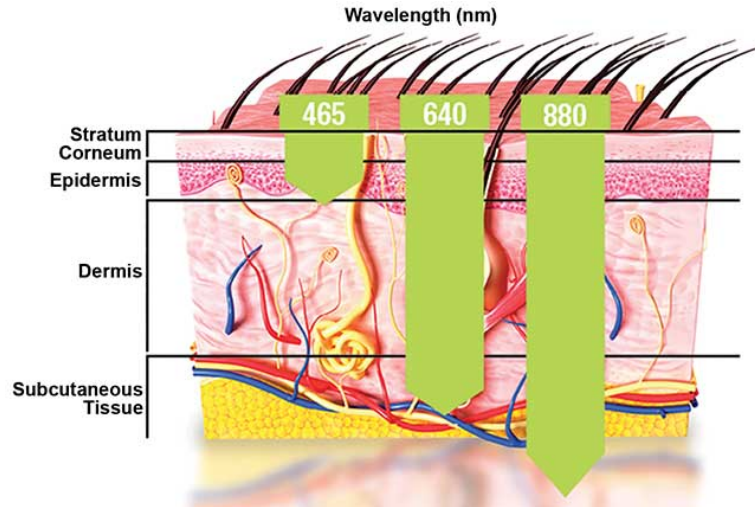
FIGURE 1: Schematic of skin layers. The stratum corneum is the tough outermost layer out of which hair is shown here. The three layers are the epidermis, the dermis and the subcutaneous tissue layer. Different wavelengths infiltrate to the different layers due to layer thickness. The green arrows show the relative depth for a given wavelength [6].

Traditional methods for treating skin injuries and wounds include solar and ultraviolet light as well as laser therapy. Light therapy utilizing LEDs is a promising technology that is less expensive, transportable and uses a relatively narrow wavelength spectrum reducing thermal damage. Hyperbaric oxygen (HBO) therapy is an approach used today to treat slow healing wounds, such as graft failures, ulcers, ischemic wounds and cell death [6]. Disadvantages of HBO therapy for treating these difficult types of wounds include the high-pressure system that some patients may not be able to tolerate. Laser light therapy has the advantage of not requiring a high-pressure system, however, these systems are limited in wavelength capabilities and beam width, thus limiting the size of the wound that can be treated. LED devices using $In_xGa_{1-x}P$ quantum well structures emitting in the range of 610nm to 650nm will enable effective wound healing for partial thickness and full thickness wounds with advantages of effectiveness, lower cost, and availability compared to traditional methods used today.

2. BACKGROUND

Light emitting diodes (LED) consists of semiconductor materials in the form of a p-n junction that emit light by means of electroluminescence. This phenomenon occurs when a sufficient amount of current is injected into the material, enabling recombination of electrons and holes. A hole is the site at which an

atom is missing an electron and is therefore positively charged. Radiative recombination of electron-hole pairs result in the release of a quanta of energy, known as photons. Non-radiative recombination degrades the efficiency of LED devices due to the lack of a released photon with the recombination of an electron-hole pair. The wavelength of the emitted light is determined by the bandgap of the semiconductor material.

Doping is the addition of impurity atoms to an intrinsic semiconductor material to create an extrinsic semiconductor with different properties. Impurity atoms are either electron donors or acceptors. Donor atoms have more valence electrons than the intrinsic semiconductor, thereby increasing the electron carrier concentration in the doped material. The resulting extrinsic semiconductor due to donor doping is called n-type. Acceptor atoms have less valence electrons, also known as more holes, than the intrinsic semiconductor. Doping with acceptor atoms increases the hole carrier concentration, resulting in an extrinsic semiconductor called p-type.

A p-n junction is the interface between p-type and n-type semiconductor material (*FIGURE 2*) [10]. The p-side of the junction has an excess hole concentration and the n-side has an excess electron concentration. In order to maintain charge neutrality at the junction, holes from the p-side diffuse to the n-side and electrons from the n-side diffuse to the p-side. Diffused holes create negative ions in the p-side and recombine with electrons to create positive ions in the n-side. Likewise, the diffused electrons create positive ions in the n-side and recombine with holes to create negative ions in the p-side. Consequently, the region around the junction is a space charge region, also known as the depletion layer.
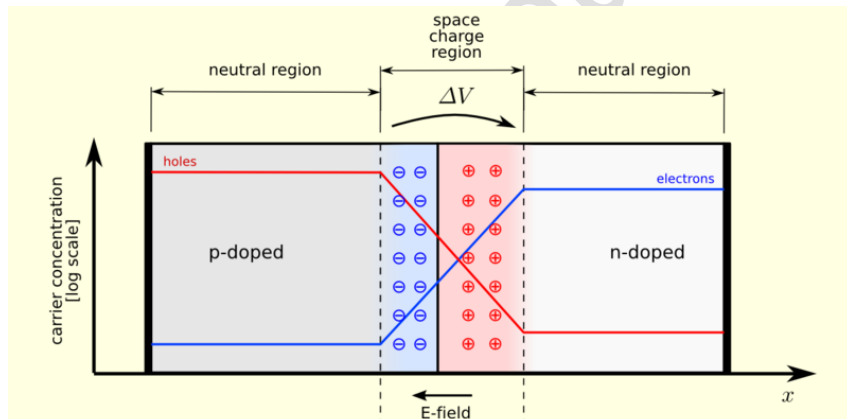
FIGURE 2: Schematic of a p-n junction. Carrier concentrations are given by a red line (holes) and a blue line (electrons). The space charge neutrality region has negative ions on the p side and positive ions on the n side [10].

At thermal equilibrium and zero applied bias, zero current flows through the device. A positive bias (forward bias) with respect to the p-side reduces the potential barrier between the two types of materials and enables current flow. A negative bias (reverse bias) increases the potential barrier and prevents current flow. A large enough negative current eventually creates breakdown where the electrons are able to tunnel through the barrier. This relationship between current and voltage is modeled by the ideal diode equation (*FIGURE 3*) [11]. I-V characteristic curves are obtainable for diode devices by measuring the current while sweeping through a voltage range.
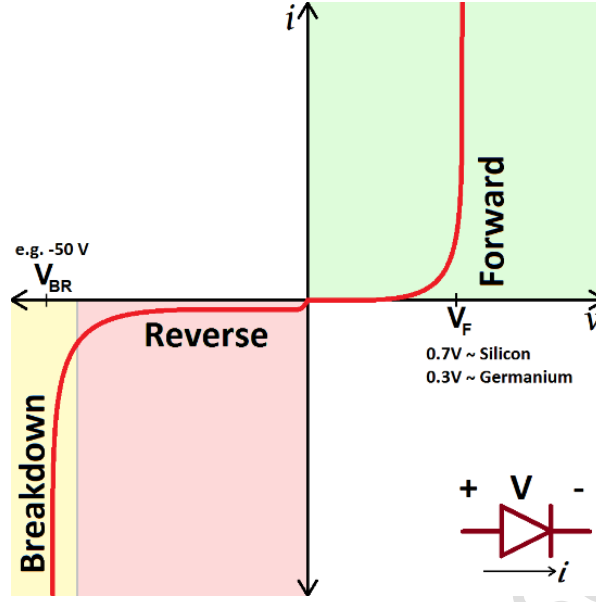
FIGURE 3: Typical I-V characteristic of a p-n junction diode. Schematic of the device is in the lower inset. The forward voltage regime has a turn-on voltage V_F and is the region of normal operation for a diode. Little current flows in the reverse region until break down voltage V_{BR} occurs [11].

The governing equations for an LED are the ideal diode equation (*EQUATION 1*) where the dark current is I_0 (*EQUATION 2*) and the current density equations (*EQUATION 3 – 4*) where both drift current and diffusion current are taken into account [12]. The electron charge is q, the potential energy is V, Boltzmann's constant is k, temperature is T, area is A, L_p and L_n are the diffusion lengths on the p and n side respectively, D_p and D_n are the p and n diffusion constants, p_n is the hole concentration on the n side, n_p is the electron concentration on the p side, μ_n is the electron mobility, μ_p is the hole mobility, and $\boldsymbol{E}$ is the electric field.

$$I = I_0(e^{\frac{qV}{kT}} - 1) \qquad\qquad\qquad EQUATION\ 1$$

$$I_0 = q\ A\ \left(\frac{D_p}{L_p}p_n + \frac{D_n}{L_n}n_p\right) \qquad\qquad\qquad EQUATION\ 2$$

$$\boldsymbol{J_n} = \boldsymbol{J_{drift}} + \boldsymbol{J_{diffusion}} = q\mu_n n\boldsymbol{E} + qD_n\nabla n \qquad\qquad\qquad EQUATION\ 3$$

$$\boldsymbol{J_p} = \boldsymbol{J_{drift}} + \boldsymbol{J_{diffusion}} = q\mu_p p\boldsymbol{E} + qD_p\nabla p \qquad\qquad\qquad EQUATION\ 4$$

3. DEVICE STRUCTURE AND SIMULATION RESULTS

In this project, Crosslight TCAD software was used to simulate the LED device using a lateral design for operation in the wavelength range of 610 to 650 nm (*FIGURE 4*). The bottom layer is n-type $(Al_{0.6}Ga_{0.4})_{0.5}In_{0.5}P$ with a donor doping of N_D=1e+18/cm^3 and thickness of 1.15 μm. The material under the n-contact is $In_{0.5}Al_{0.5}P$ with donor doping of N_D=1e+20/cm^3 and thickness of 0.15 μm. The final part of

the n-side of the device is again n-type $(Al_{0.6}Ga_{0.4})_{0.5}In_{0.5}P$ with a donor doping of N_D=1e+18/cm^3 and thickness of 0.15 μm.

The active region of the structure consists of $In_xGa_{1-x}P$ multiple quantum wells (MQW) with and $(Al_{0.6}Ga_{0.4})_{0.5}In_{0.5}P$ barriers. The barriers and wells both have donor doping of N_D=1e+16/cm^3. The material effects studied in this project include well composition, well number and well thickness. Indium composition of the wells is varied between 40 – 70%. The thickness of the quantum wells studied are 5 nm, 10 nm and 15 nm while maintaining a barrier thickness of 15 nm. The number of wells studied range from 1 to 10. The analysis of these effects are discussed below. Above the MQW active region is p-type $(Al_{0.6}Ga_{0.4})_{0.5}In_{0.5}P$ with a acceptor doping of N_A=1e+19/cm^3 and thickness of 1.3 μm. This layer is followed by p-$In_{0.5}Al_{0.5}P$ with acceptor doping of N_A=1e+20/cm^3 and finally by the p-contact.
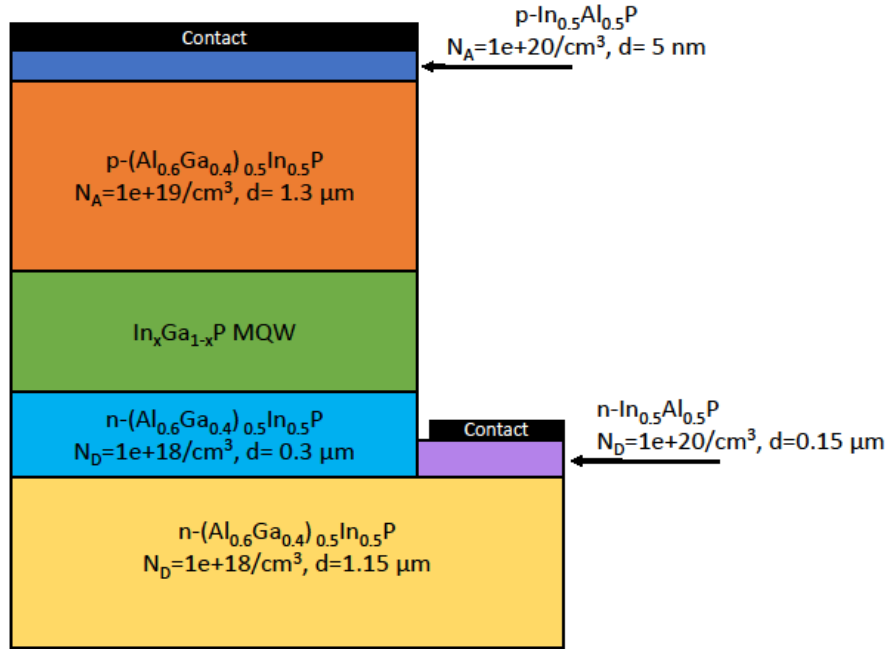
FIGURE 4: Design of the lateral LED simulated. Each layer is labeled with the material above. The donor concentrations N_D and the acceptor concentrations N_A are included for each layer as well as the layer thickness d. The multiple quantum well (MQW) active region consist of $In_xGa_{1-x}P$ wells and $(Al_{0.6}Ga_{0.4})_{0.5}In_{0.5}P$ barriers.

Effect of indium composition of multiple quantum wells

The energy levels for a finite quantum well are found by solving Schrödinger's equation as seen in *EQUATION 5* where ℏ is Planck's constant, m is the effective mass, $V(x)$ is the potential energy, ψ is the electron wave function and E is the energy [13]. By setting the potential energy $V(x) = 0$ inside of the quantum well, this equation reduces to *EQUATION 6*.

$$\frac{-\hbar^2}{2m}\frac{d^2\psi}{dx^2} + V(x)\psi = E\psi \qquad\qquad EQUATION\ 5$$

$$\frac{-\hbar^2}{2m}\frac{d^2\psi}{dx^2} = E\psi \qquad\qquad EQUATION\ 6$$

5

Letting $k = \sqrt{2mE}/\hbar$ we can solve for energy. This results in the emission energy for a finite quantum well inversely proportional to the effective mass as seen in *EQUATION 7*.

$$E = \frac{k^2\hbar^2}{2m}$$

EQUATION 7

Energy is also related to the emitted wavelength by the relation $E = hc/\lambda = 1240/\lambda$ where λ is in nm. Therefore, increasing the effective mass in the quantum well will decrease the emission energy which is related to an increase in emission wavelength. *FIGURE 5* demonstrates this relation. The study of indium composition holds the number of quantum wells constant at 5 wells and the well and barrier thicknesses are each 5 nm. By increasing the indium composition, the effective mass is increased. The indium composition in the well is increased from 40 – 70%. The emission wavelength is tuned between 614 nm for an indium composition of 40% to 720 nm for an indium composition of 70%.
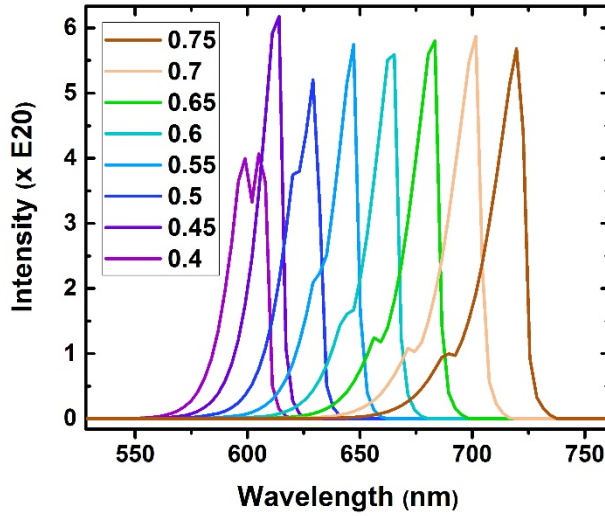
FIGURE 5: Emission intensity versus wavelength for different compositions of indium in the quantum well. Emission wavelength increases with increase in indium composition. Number of quantum wells held constant at 5 with well width and barrier widths of 5 nm. Arbitrary units on y-axis.

The I-V characteristic curves are portrayed in *FIGURE 6* for indium composition between 40 – 70%. In general, the turn-on voltage increases as the bandgap of the semiconductor material increases. Increasing the composition of indium increases the effective mass, thereby decreasing the bandgap. *FIGURE 6* is in agreement with this expected trend. As the indium composition increases, the turn-on voltage decreases. Lower values for the turn on voltage are ideal because this means that lower power is necessary for the device operation. However, there is a trade-off with the emission wavelength. The shorter

the wavelength, the lower the LED will infiltrate the layers of skin for wound healing and the higher the turn-on voltage required for operation.
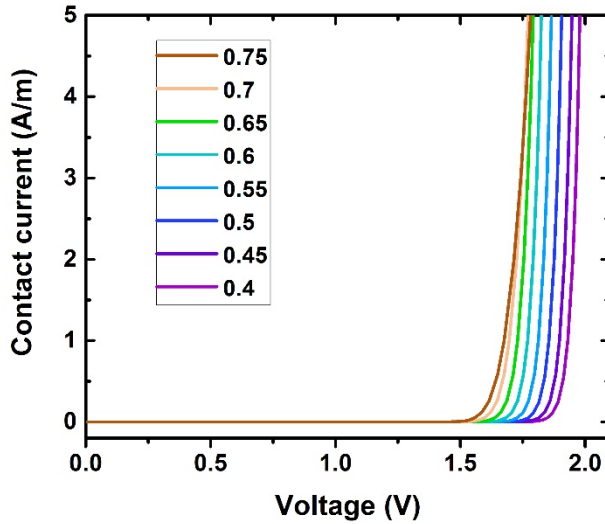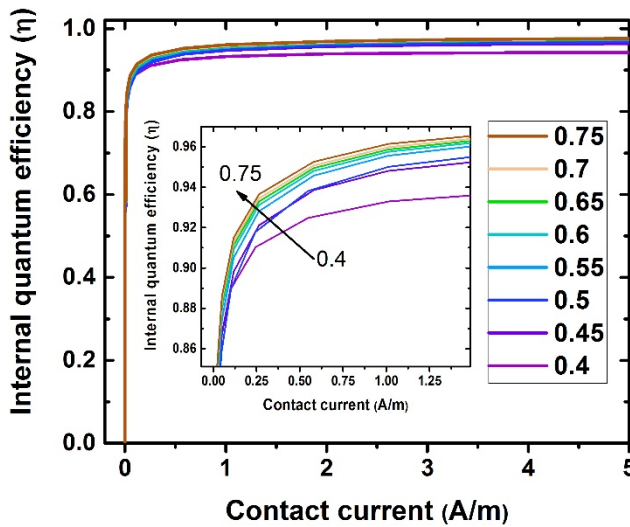

FIGURE 6: I-V characteristic for different compositions of indium in the quantum well. Turn-on voltage increases with decrease in indium composition. Number of quantum wells held constant at 5 with well width and barrier widths of 5 nm.

Internal quantum efficiency is dependent on the radiative lifetime τ_r and the non-radiative lifetime τ_{nr} as seen in *EQUATION 8* [15]. *FIGURE 7* demonstrates that by increasing the indium composition from 40 – 70%, the internal quantum efficiency increases. The inset of FIGURE is a zoomed in image and better illustrates this increase in internal quantum efficiency. Compositions between 55-75% have much closer internal quantum efficiency values relative to each other. Thus, optimization of this device should have a composition within this range.

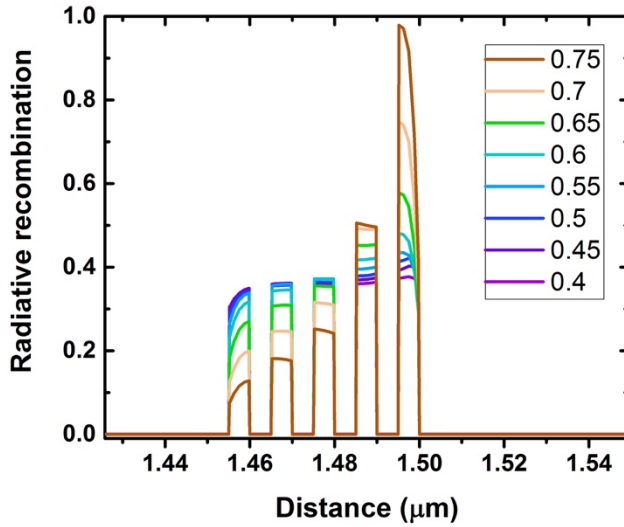$$\eta_{int} = \frac{\tau_{nr}}{\tau_r + \tau_{nr}} \hspace{4cm} EQUATION\ 8$$

FIGURE 7: Internal quantum efficiency for different compositions of indium in the quantum well. Internal quantum efficiency increases with increase in indium composition. Inset is a zoomed in image to better show trend. Number of quantum wells held constant at 5 with well width and barrier widths of 5 nm.

Furthermore, the indium composition affects the radiative recombination. *FIGURE 8* demonstrates that as the indium composition increases, the distribution of the radiative recombination shifts. At 40% indium the

distribution of the radiative recombination is constant throughout the 5 quantum wells For the case of 75% indium, the far right quantum well has the most radiative recombination and the far left well has the least. However, the area under all of the curves remains the same for each case.


FIGURE 8: Radiative recombination for different compositions of indium in the quantum well. The total area under each curve remains constant. Number of quantum wells held constant at 5 with well width and barrier widths of 5 nm.

Based on these results, the indium composition of 55% is best suited for wound healing due to its emission wavelength of 647 nm, moderate turn-on voltage of approximately 1.65V and its high internal quantum efficiency. There is a trade-off with this composition with radiative recombination. Larger values of radiative recombination are achievable for 75% composition; however, the corresponding emission wavelength is well out of the target range of 610 – 650 nm.
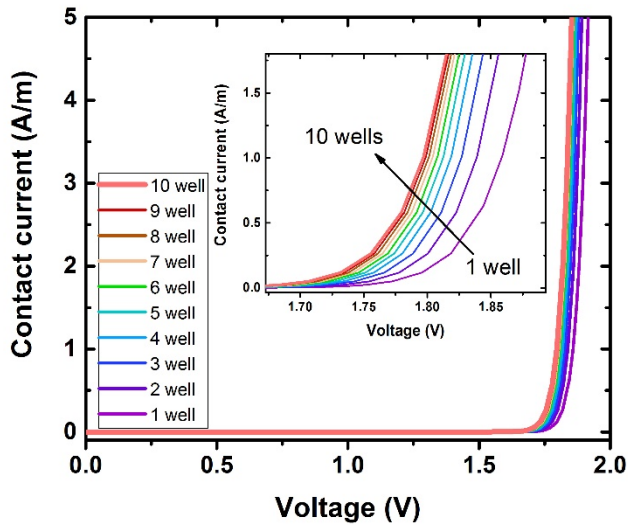
Effect of the number of quantum wells

The number of quantum wells in the active region are studied while maintaining the indium composition at 55% and the well and barrier widths at 5 nm. By increasing the number of quantum wells, the number of regions that can emit photons increases. Therefore, it is expected that as the number of quantum increases, the emission peak wavelength intensity will also increase. *FIGURE 9* demonstrates this behavior. There is a significant increase between 1 and 2 quantum wells, after which other trade-offs must be considered.
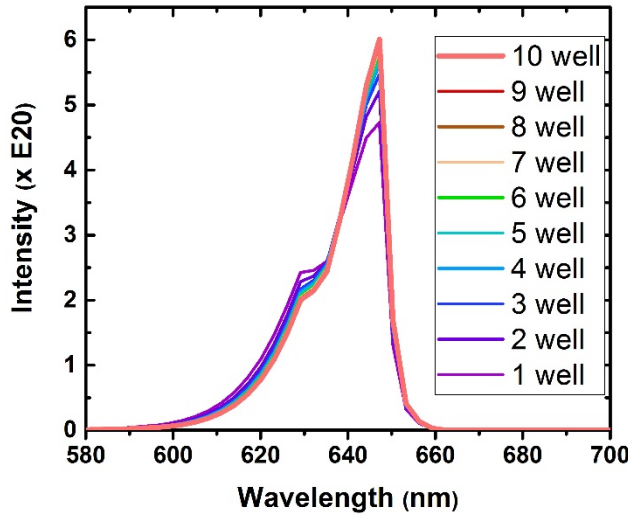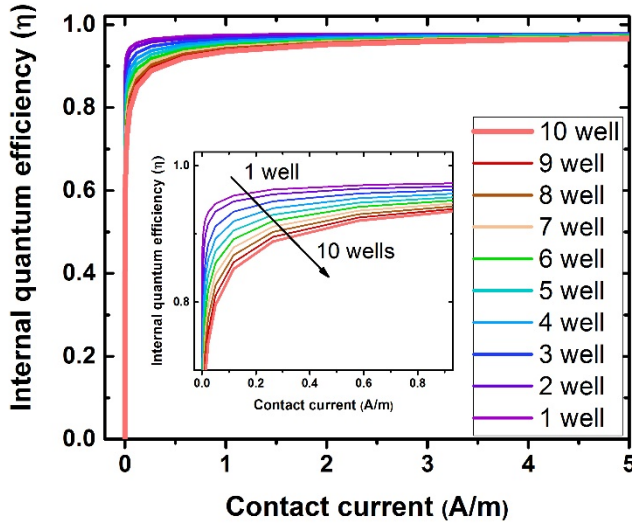
FIGURE 9: Emission spectra for different number of quantum wells. Emission wavelength remains constant while intensity increases with increasing the number of quantum wells in the active region. Quantum well composition held constant at 55% indium with well and barrier widths of 5 nm.

FIGURE 10 indicates a reduction in the turn-on voltage as the number of quantum well increases. However, upon zooming in, as seen in the inset, the reduction is not very significant. Optimizing the turn-on voltage would require the number of quantum wells to be between 4 – 10 wells.


FIGURE 10: I-V characteristic for different number of quantum wells. Turn-on voltage decreases with increasing the number of quantum wells in the active region. Inset is a zoomed in image to better show trend. Quantum well composition held constant at 55% indium with well and barrier widths of 5 nm.

The internal quantum efficiency is affected by the number of quantum wells (*FIGURE 11*). A single quantum well has internal quantum efficiency approximately 98% at 1 mA, however, 10 quantum wells reduces the internal quantum efficiency to approximately 83% at 1 mA. Increasing the number of quantum wells increases the overall resistance and thus a decrease in the internal quantum efficiency is expected.

9

FIGURE 11: Internal quantum efficiency for different number of quantum wells. Internal quantum efficiency decreases with increasing the number of quantum wells in the active region. Inset is a zoomed in image to better show trend. Quantum well composition held constant at 55% indium with well and barrier widths of 5 nm.

The distribution of radiative recombination is evenly distributed throughout the systems of multiple quantum wells (*FIGURE 12)*. The amount of radiative recombination from a single quantum well is approximately equal to the sum of all of the wells in each case. Optimizing the number of wells must take into account the small emission intensity for lower number of quantum wells even though the internal quantum efficiency is higher. Furthermore, a lower number of quantum wells also increase the turn-on voltage. Thus, 5 quantum wells is proposed. The emission intensity does not increase significantly for more than 5 quantum wells nor does the radiative recombination. Furthermore, the turn-on voltage is moderate while maintaining a relatively high internal quantum efficiency.
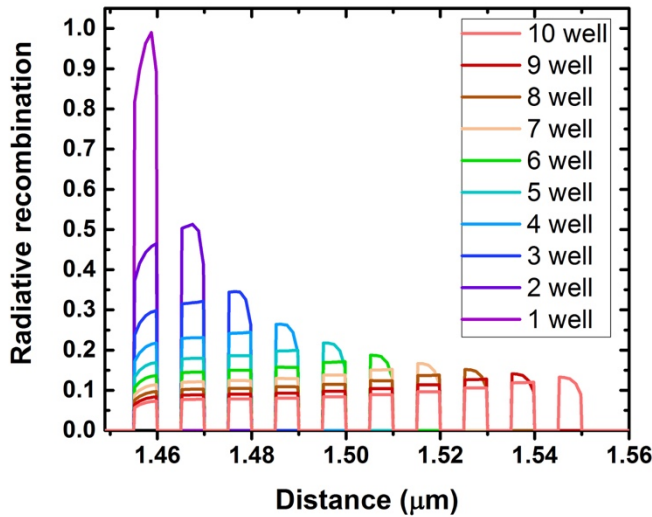

FIGURE 12: Radiative recombination for different number of quantum wells. The total area under each curve remains constant. The total radiative recombination for 1 well is divided amongst the multiple wells. Quantum well composition held constant at 55% indium with well and barrier widths of 5 nm.

10

Effect of multiple quantum well thickness

The well thickness is studied for a single quantum well while maintaining the indium composition at 55% and the barrier thickness at 15 nm. The energy levels in an infinite quantum well are related to the well thickness as seen in *EQUATION 9* where n is the energy level, $\hbar$ is Planck's constant, m is the effective mass and a is the width of the well.

$$E_n = \frac{n^2 \pi^2 \hbar^2}{2\,m\,a^2}$$

EQUATION 9

A finite quantum well can be approximated by the infinite well case by noting that the energy levels are slightly lower for the finite well case compared to the infinite well. Since energy is inversely proportional to the width of the well, it is expected that increasing the well width will decrease the emission energy and thereby increase the emission wavelength. The well thicknesses studied here are 5 nm, 10 nm and 15 nm. *FIGURE 13* demonstrates that thicker wells reduces the emission intensity as well as red-shift the emission wavelength.
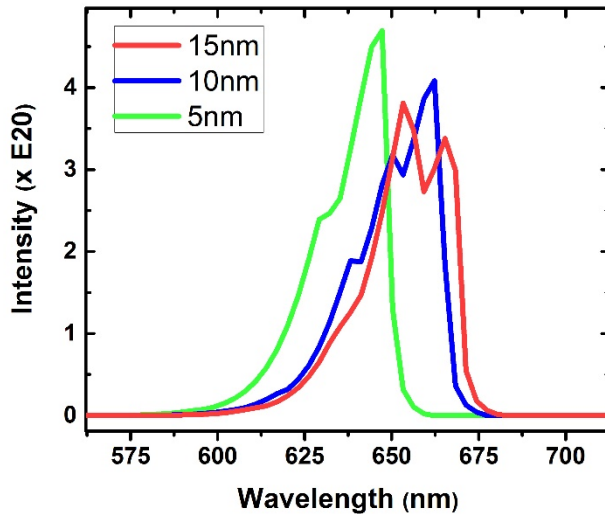

FIGURE 13: Emission spectra for different thicknesses for a single quantum well. Emission wavelength is red-shifted for increasing well thickness. Single quantum well composition held constant at 55% and barrier widths of 15 nm.

A lower energy is also related to a lower turn-on voltage. *FIGURE 14* portrays the 15 nm quantum well to has a turn-on voltage of approximately 1.7 V while the 5 nm quantum well has a turn-on voltage of approximately 1.8 V.
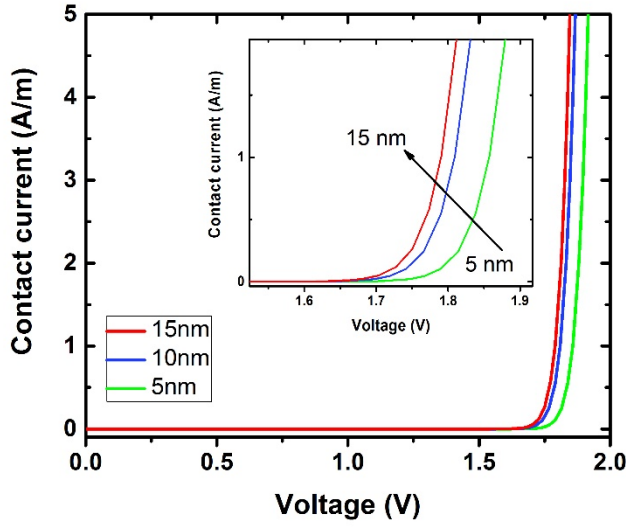
FIGURE 14: I-V characteristic for different thicknesses of a single quantum well. Turn-on voltage decreases with increasing the width. Inset is a zoomed in image to better show trend. Single quantum well composition held constant at 55% and barrier widths of 15 nm.

The internal quantum efficiency slightly decreases with increasing the width of the well (*FIGURE 15*). This increase is only slight for 1 quantum well, however, the effect may become more pronounced for increasing the number of quantum wells due to increasing the total resistance of the system. For the case of 1 quantum well, the thickness is not a significant optimization parameter on the internal quantum efficiency.
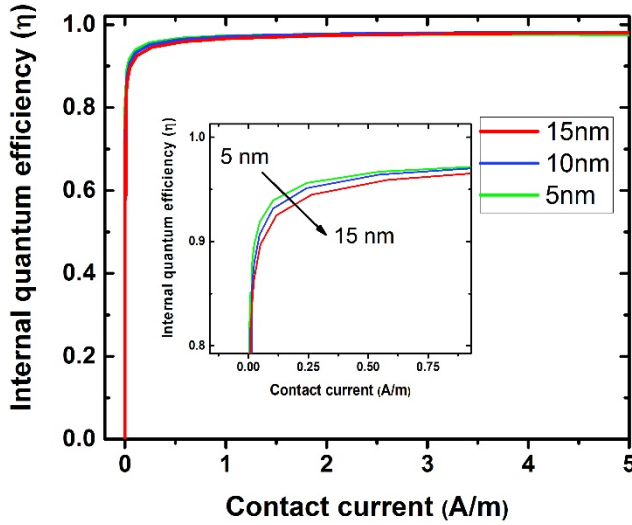
FIGURE 15: Internal quantum efficiency for different thicknesses of a single quantum well. Internal quantum efficiency decreases with increasing the width. Inset is a zoomed in image to better show trend. Single quantum well composition held constant at 55% and barrier widths of 15 nm.

The total area under each curve in the radiative recombination plot of *FIGURE 16* is constant for each well thickness case. Optimizing the thickness of the quantum wells is thus chosen to be 5 nm due to the system's better confinement of electrons.

12
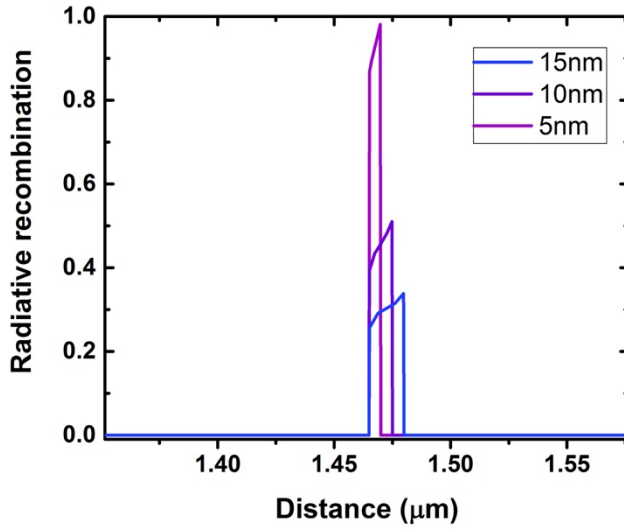
FIGURE 16: Radiative recombination for different thicknesses of a single quantum well. The total area under each curve remains constant. Single quantum well composition held constant at 55% and barrier widths of 15 nm.

Final proposed structure

The final structure uses an optimized indium composition of 55% and 5 quantum wells with thickness of 5 nm. *FIGURE 17* portrays the band diagram of this device with the 5 quantum wells visible.
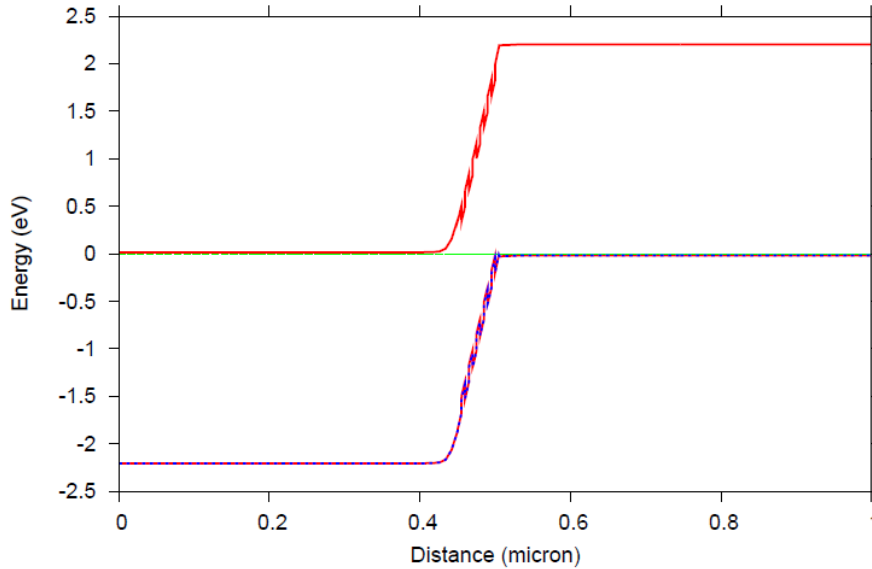

FIGURE 17: Final structure band diagram. Indium composition is 55% with 5 quantum wells. Widths and barriers are 5 nm.

The selected indium composition results in a peak emission wavelength of 647 nm as seen in *FIGURE 18*. The I-V characteristic shows a turn-on voltage of approximately 1.8 V and the internal quantum efficiency is greater than 95% as portrayed in *FIGURE 19*.
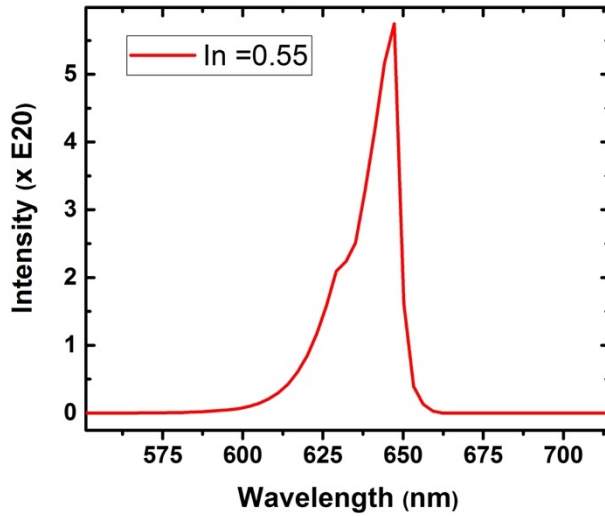
FIGURE 18: Final structure emission intensity versus wavelength. Peak wavelength is 647 nm. Indium composition is 55% with 5 quantum wells. Widths and barriers are 5 nm.
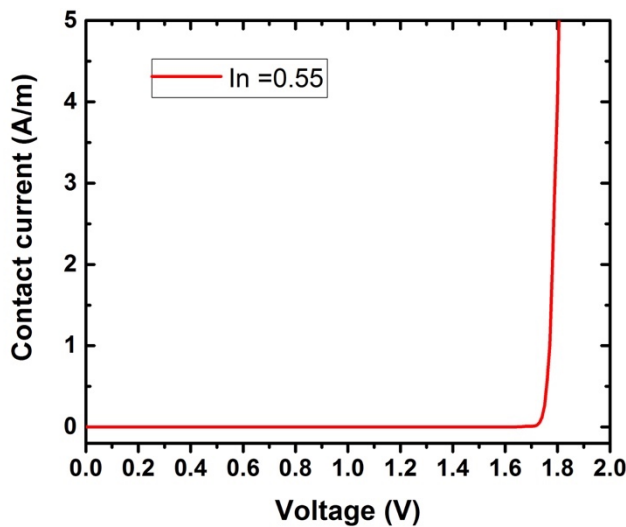
FIGURE 19: Final structure I-V characteristic. Turn on voltage approximately 1.8 V. Indium composition is 55% with 5 quantum wells. Widths and barriers are 5 nm.

Current is plotted as a vector function throughout the device in *FIGURE 20*. Current crowding effects may be observed for this structure. Doping in the layers below the p-contact maintain a constant vector field. Doping in the n-type material maintain a relatively uniform current vector field, with a slight reduction in the bottom left corner. This is a minimal reduction and does not affect the results significantly.
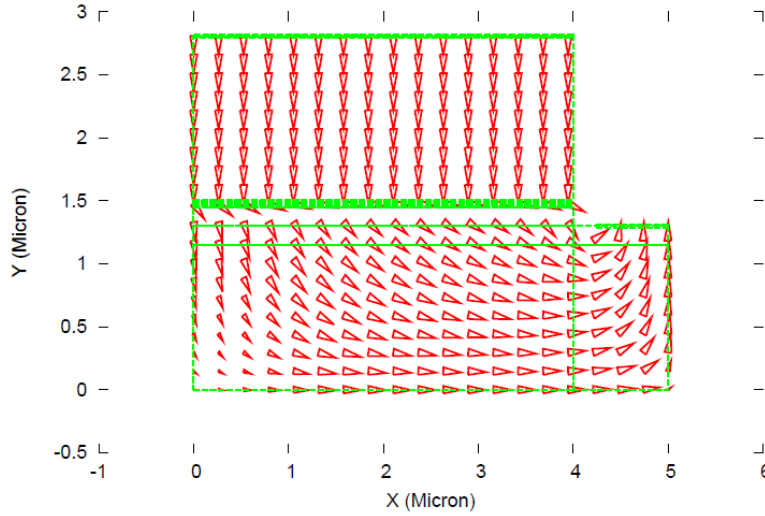
FIGURE 20: Current plotted as vector function in final structure. No significant current crowding. Indium composition is 55% with 5 quantum wells. Widths and barriers are 5 nm.

4. SUMMARY AND CONCLUSIONS

Difficult to heal wounds require the assistance of innovative technology. Treatment of skin wounds using light therapy enables flexibility in tuning the wavelength to correspond to the type of wound. Injuries to the epidermis layer of the skin are the shallowest wound and are treatable with blue wavelengths. Injuries to the dermis and subcutaneous tissue skin layers as either partial thickness wounds or full thickness wounds are difficult to heal and require longer wavelengths. Wavelengths in the range of 610 – 650 nm are particularly of interest due to reaching the dermis as well as the subcutaneous tissue layer.

LEDs are the preferable source of light for light therapy wound healing. Ultraviolet as well as solar light sources are damaging to the skin due to over thermal exposure to the cells. Non-ablative lasers do not expose skin cells to excess thermal energy, however, drawbacks to this system include high expenses, high maintenance and are not mobile systems. LEDs are convenient systems with a relatively narrow wavelength for targeting specific layers of the skin for healing.

The LED structure considered in this proposal is a lateral design with $In_xGa_{1-x}P$ multiple quantum wells and $(Al_{0.6}Ga_{0.4})_{0.5}In_{0.5}P$ barriers. The indium composition of the quantum wells is tuned between 40 – 70%. The emitted wavelength increases from 614 nm for 40% indium to 720 nm for 70% indium. An optimized composition value of 55% indium is chosen due to the moderate turn-on voltage, moderate radiative recombination and high internal quantum efficiency relative to the other compositions. The number of quantum wells in the active region studied range from 1 – 10 wells. Internal quantum efficiency decreases even though the emission intensity increases as the number of wells increases. An LED structure with 5 quantum wells is optimal due to a high internal quantum efficiency and a high emission wavelength intensity achieved simultaneously. The well thickness is studied at 5 nm, 10 nm and 15 nm for a single well while maintaining a barrier thickness of 15 nm. The emission wavelength increases while the intensity decreases for increasing the well thickness. The internal quantum efficiency is high for all three values of well thickness. Optimization of these parameters will increase the effectiveness of light therapy for patients afflicted with skin wounds and injuries.

REFERENCES

1. T. Fushimi, S. Inui, T. Nakajima, M. Ogasawara, K. Hosokawa, and S. Itami, "Green light emitting diodes accelerate wound healing: Characterization of the effect and its molecular basis in vitro and in vivo," Wound Rep Reg 20 226 (2012).
2. W. Posten, D. A. Wrone, J. S. Dover, K. A. Arndt, S. Silapunt, and M. Alam, "Low-level laser therapy for wound healing: mechanism and efficacy," Dermatol Surg 31 (3) 334 (2005).
3. F. M. Hendriks, D. Brokken, C. W. J. Oomens, D. L. Bader, and F. P. T. Baaijens, "The relative contributions of different skin layers to the mechanical behavior of human skin in vivo using suction experiments," Medical Engineering & Physics 28 259 (2006).
4. M. E. de Abreu Chaves, A. R. de Araújo, A. C. C. Piancastelli, and M. Pinotti, "Effects of low-power light therapy on wound healing: Laser x LED," An Bras Dermatol. 89 (4) 616 (2014).
5. H. T. Whelan, R. L. Smits, E. V. Buchman, N. T. Whelan, S. G. Turner, D. A. Margolis, V. Cevenini, H. Stinson, R. Ignatius, T. Martin, J. Cwiklinski, A. F. Philippi, W. R. Graf, B. Hodgson, L. Gould, M. Kane, G. Chen, and J. Caviness, "Effect of NASA light-emitting diode irradiation on wound healing," J. Clinical Laser Med. & Surg. 19 (6) 305 (2001).
6. BioPhotas. (2015). Retrieved April 22, 2018, from https://proskinguru.com/wp-content/uploads/2015/03/photo.jpg
7. P. Martin, "Wound healing – Aiming for perfect skin regeneration," Science 276 75 (1997).
8. N. Adamskaya, P. Dungel, R. Mittermayr, J. Hartinger, G. Feichtinger, K. Wassermann, H. Redl, and M. van Griensven, "Light therapy by blue LED improves wound healing in an excision model in rats," Injury, Int. J. Care Injured 42 917 (2011).
9. K. Zulkowski, "Wound terms and definitions," WCET Journal 35 (1) 22 (2015).
10. P–n junction. (2018, April 14). Retrieved April 22, 2018, from https://en.wikipedia.org/wiki/P%E2%80%93n_junction#/media/File:Pn-junction-equilibrium-graphs.png
11. Sparkfun. (n.d.). Diodes. Retrieved April 22, 2018, from https://learn.sparkfun.com/tutorials/diodes/real-diode-characteristics
12. B. G. Streetman, and S. Banerjee, Solid State Electronic Devices, Boston: Pearson, (2016).
13. D. Griffiths, Introduction to Quantum Mechanics, 2nd edition, Pearson Prentice Hall, (2004).